Multi-twist retarders: broadband retardation control using self-aligning reactive liquid crystal layers

Ravi K. Komanduri, Kristopher F. Lawler, and Michael J. Escuti*

Department of Electrical and Computer Engineering, North Carolina State University, Raleigh, NC, 27695 USA

*mjescuti@ncsu.edu

Abstract: We report on a family of complex birefringent elements, called Multi-Twist Retarders (MTRs), which offer remarkably effective control of broadband polarization transformation. MTRs consist of two or more twisted liquid crystal (LC) layers on a single substrate and with a single alignment layer. Importantly, subsequent LC layers are aligned directly by prior layers, allowing simple fabrication, achieving automatic layer registration, and resulting in a monolithic film with a continuously varying optic axis. In this work, we employ a numerical design method and focus on achromatic quarter- and half-wave MTRs. In just two or three layers, these have bandwidths and general behavior that matches or exceeds all traditional approaches using multiple homogenous retarders. We validate the concept by fabricating several quarter-wave retarders using a commercial polymerizeable LC, and show excellent achromaticity across bandwidths of 450-650 nm and 400-800 nm. Due to their simple fabrication and many degrees of freedom, MTRs are especially well suited for patterned achromatic retarders, and can easily achieve large bandwidth and/or low-variation of retardation within visible through infrared wavelengths.

© 2013 Optical Society of America

OCIS codes: (260.5430) Polarization; (160.3710) Liquid crystals; (310.4165) Multilayer design; (310.010) Thin films; (310.6805) Theory and design.

References and links

1. D. H. Goldstein, *Polarized Light* (CRC Press, 2011), 3rd ed.
2. H. Mattoussi, M. Srinviasarao, P. Kaatz, and G. C. Berry, "Birefringence and dispersion of uniaxial media," Mol. Cryst. and Liq. Cryst. **223**, 69–84 (1992).
3. O. Parri, G. Smith, R. Harding, H. Yoon, I. Gardiner, J. Sargent, and K. Skjonnemand, "Patterned retarder films using reactive mesogen technology," Proc. SPIE **7956**, 1–11 (2011).
4. D. Clarke, "Achromatic halfwave plates and linear polarization rotators," Opt. Acta **14**, 343–350 (1967).
5. P. Hariharan, "Achromatic and apochromatic halfwave and quarterwave retarders," Opt. Eng. **35**, 3335–3337 (1996).
6. J. Schirmer and T. Schmidt-Kaler, "Liquid crystal phase retarder with broad spectral range," Opt. Commun. **176**, 313–317 (2000).
7. B. Boulbry, B. Bousquet, B. Le Jeune, Y. Guern, and J. Lotrian, "Polarization errors associated with zero-order achromatic quarter-wave plates in the whole visible spectral range," Opt. Exp. **9**, 225–235 (2001).
8. M. G. Destriau and J. Prouteau, "Realisation dun quart donde quasi achromatique par juxtaposition de 2 lames cristallines de meme nature," J. Phys. Radium **10**, 53–55 (1949).
9. S. Pancharatnam, "Achromatic combinations of birefringent plates. Part I. An achromatic circular polarizer," Proc. Ind. Acad. Sci. A **41**, 130–136 (1955).

#176332 - $15.00 USD Received 17 Sep 2012; revised 30 Nov 2012; accepted 3 Dec 2012; published 4 Jan 2013
(C) 2013 OSA

10. S. Pancharatnam, "Achromatic combinations of birefringent plates. Part II. An achromatic quarter-wave plate," Proc. Ind. Acad. Sci. A **41**, 137–144 (1955).
11. A. Samoylov, V. Samoylov, A. Vidmachenko, and A. Perekhod, "Achromatic and super-achromatic zero-order waveplates," J. Quant. Spectrosc. Radiat. Transfer **88**, 319–325 (2004).
12. C. M. McIntyre and S. E. Harris, "Achromatic wave plates for visible spectrum," J. Opt. Soc. Am. **58**, 1575–1580 (1968).
13. S. Tang and H. Kwok, "Mueller calculus and perfect polarization conversion modes in liquid crystal displays," J. Appl. Phys. **89**, 5288–5294 (2001).
14. K. Yoon, H. Yoon, K. Kim, H. Cui, J. Park, W. Jang, and O. Park, "Application of twisted retarders to a cholesteric liquid crystal polarizer for the control of output polarization states," Jap. J. Appl. Phys. **48**, 1–6 (2009).
15. O. Parri, K. Skjonnemand, K. Slaney, and M. Verrall, "Combination of optical films comprising a twisted a-plate and a polarizer," US Patent **7,187424** (2007).
16. M. Lavrentovich, T. Sergan, and J. Kelly, "Switchable broadband achromatic half-wave plate with nematic liquid crystals," Opt. Lett. **29**, 1411–1413 (2004).
17. Z. Zhuang, Y. Kim, and J. Patel, "Achromatic linear polarization rotator using twisted nematic liquid crystals," Appl. Phys. Lett. **76**, 3995–3997 (2000).
18. T. X. Wu, Y. Huang, and S.-T. Wu, "Design optimization of broadband linear polarization converter using twisted nematic liquid crystal," Jap. J. Appl. Phys. **42**, L39–L41 (2003).
19. S. Shen, J. She, and T. Tao, "Optimal design of achromatic true zero-order waveplates using twisted nematic liquid crystal," J. Opt. Soc. Am. A **22**, 961–965 (2005).
20. D. Clarke, "Interference effects in Pancharatnam wave plates," J. Opt. A - Pure Appl. Opt. **6**, 1047-1051 (2004).
21. R. Komanduri, J. Kim, K. Lawler, and M. Escuti, "Multi-twist retarders for broadband polarization transformation," Proc. SPIE **8279**, 1–10 (2012).
22. J. Kim, R. Komanduri, K. Lawler, D. Kekas, and M. Escuti, "Efficient and monolithic polarization conversion system based on a polarization grating," Appl. Opt. **51**, 4852–4857 (2012).
23. Y. Li, J. Kim, and M. Escuti, "Broadband orbital angular momentum manipulation using liquid crystal thin films," Proc. SPIE **8274**, 1–8 (2012).
24. D. Mawet, "Taking the vector vortex coronagraph to the next level for ground- and space-based exoplanet imaging instruments: review of technology developments in the usa, japan, and europe," Proc. SPIE **8151**, 1–14 (2011).
25. C. Oh and M. Escuti, "Achromatic diffraction from polarization gratings with high efficiency," Opt. Lett. **33**, 2287–2289 (2008).
26. D. Broer and I. Heynderickx, "3 dimensionally ordered polymer networks with a helicoidal structure," Macromolecules **23**, 2474–2477 (1990).
27. S. Kelly, "Anisotropic networks," J. Mater. Chem. **5**, 2047–2061 (1995).
28. M. Schadt, H. Seiberle, A. Schuster, and S. M. Kelly, "Photo-induced alignment and patterning of hybrid liquid-crystalline polymer films on single substrates," Jap. J. Appl. Phys. **34**, L764–L767 (1995).
29. D. Broer, J. Lub, and G. Mol, "Wide-band reflective polarizers from cholesteric polymer networks with a pitch gradient," Nature **378**, 467–469 (1995).
30. C. J. Koester, "Achromatic combinations of half-wave plates," J. Opt. Soc. Am. **49**, 405–409 (1959).

1. Introduction

Retarders are birefringent elements that can transform polarization by inducing different phase shifts between orthogonal electric-field components of electromagnetic waves. Also called wave plates, they are useful nearly anywhere that polarization [1] is important. The simplest retarders, formed by a homogeneous uniaxial birefringence Δn with a thickness d, have a phase retardation $\Gamma = 2\pi\Delta nd/\lambda$ that varies strongly with wavelength λ.

Broadband (including achromatic) polarization transformation that can be precisely controlled over a broad range of wavelengths is especially important in applications that involve human perception or multiple simultaneous channels at different wavelengths. Unfortunately, the spectral dispersion of the birefringence $\Delta n(\lambda)$ of nearly all optical materials [2] does not in general enable this within one plate; an exception [3] will be discussed later. Instead, several techniques involving multiple birefringent plates have been developed that achieve broadband behavior via the principle of retardation compensation, where a deficiency in the retardation of one plate is at least partially corrected by a subsequent plate.

A first approach [4–6] employs at least two homogeneous plates of different materials (*i.e.*, Δn) and d, usually arranged with orthogonal optical axes (Fig. 1(a)). This depends on having

#176332 - $15.00 USD Received 17 Sep 2012; revised 30 Nov 2012; accepted 3 Dec 2012; published 4 Jan 2013
(C) 2013 OSA

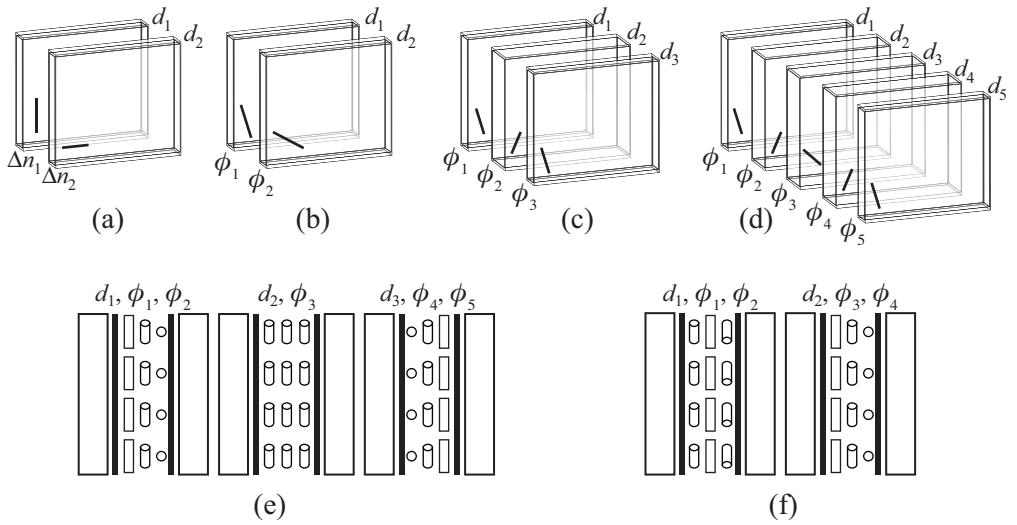

Fig. 1. Representative prior achromatic retarder approaches. Some use homogenous plates with (a) different materials [4], and others use a single material in designs with (b) two [8] (DP), (c) three [9] (Pancharatnam), and (d) five [11] (APSAW) elements. Some others use two twisted liquid crystal (LC) elements, (e) with [16] and (f) without [19] an additional element, having six and four substrates with LC alignment layers, respectively.

an appropriate difference $\Delta n_2(\lambda)d_2 - \Delta n_1(\lambda)d_1$, which is certainly attainable (*e.g.*, quartz and MgF_2), but leads to a limited achromatic bandwidth and is strongly sensitive to alignment errors [7], temperature variations, and incidence angle.

A second approach employs multiple homogeneous plates of the same material, wherein their optical axis orientations ϕ and individual d are not usually orthogonal or otherwise trivial. The simplest case [8], introduced by Destriau and Prouteau (DP), involves just two plates (Fig. 1(b)), but was generalized and improved by Pancharatnam [9] for three plates, including the popular QHQ design [10] (Fig. 1(c)). The principle can be extended further [6,11,12], so that additional retarders (Fig. 1(d)) allow for almost arbitrarily wide achromatic bandwidths in principle. In practice, however, since each plate must be formed on its own as a physically separate element and subsequently aligned, small errors in ϕ and d of each become exponentially deleterious.

Note the underlying principle throughout: broadband polarization transformation is achieved through additional degrees of freedom arising from using multiple homogeneous retarders, which have an optical axis varying discontinuously through the compound structure. This may be extended to *single* inhomogenous birefringent layers as well, with a continuously varying optical axis. In a way, this is the essence of liquid crystal (LC) displays of all kinds, especially the twisted modes [13], which transform linear to near-linear polarizations. The attempts to use a single twisted LC layer [14,15] explicitly as a broadband (quarter-wave) retarder show some, but rather limited, achromatic behavior.

A third approach may therefore be identified, employing *multiple* (but separate) twisted LC elements. The few examples involve twisted LC cells combined with homogenous LC cells, to form a switchable achromatic half-wave retarder [16] (Fig. 1(e)), polarization rotator [17, 18], and quarter-wave retarder [19] (Fig. 1(f)). These all suffer from fabrication complications similar to the previous approaches, due to the multiple elements fabricated individually and subsequently aligned, and are magnified further since each LC element is expressly envisioned with two substrates and two LC alignment layers (with their own alignment challenges).

#176332 - $15.00 USD Received 17 Sep 2012; revised 30 Nov 2012; accepted 3 Dec 2012; published 4 Jan 2013
(C) 2013 OSA

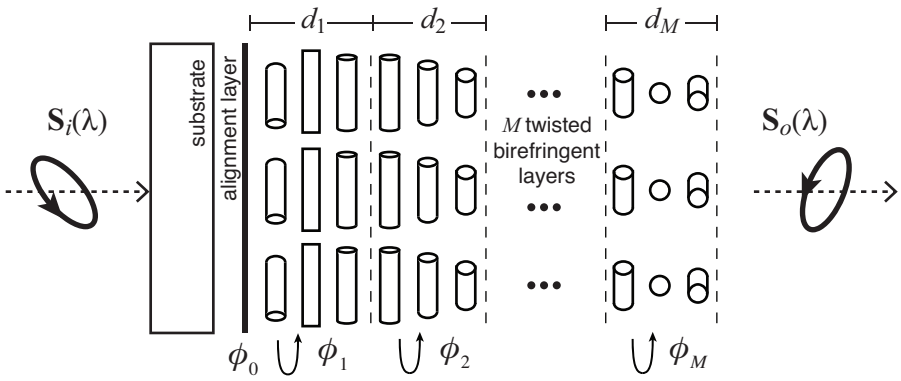

Fig. 2. Illustration of the multi-twist retarder (MTR) monolithic structure, with one substrate and alignment layer, and M twisted layers. Cylinders correspond to the optical axis (and the nematic director field). Subsequent layers are aligned by the prior one.

Therefore, even though the work to date using this third approach hints at some useful broadband control, it is nearly overwhelmed by the complexity of so many substrates and alignment layers and the resulting alignment challenges. Also, such multiple elements lead to undesirable reflections [20] due to the discontinuous optical axis that may be of relevance to some applications including interferometry etc. Furthermore, no one has yet offered a general treatment of the approach, examined designs beyond the limited specific twist angles and layers reported in the prior work [16, 17, 19], or studied the blended relationship between retardation and rotation that occurs when using multiple twisted layers. We aim to address all of these in this work, substantially expanding and formalizing beyond our initial report [21], by developing a general theoretical framework to design broadband retarders for arbitrary polarization transformation, identifying the optimal achromatic designs for the first time, and including substantially more fabrication details and experimental results.

2. Multi-twist retarder (MTR) concept

Here, we describe a family of broadband retarders, using *multiple* twisted LC layers on a *single* alignment layer and substrate (Fig. 2), called multi-twist retarders (MTRs). Its most important feature is that subsequent LC layers are directly aligned by previous ones, resulting in simple fabrication and a *monolithic* film, that is capable of retardation control for nearly arbitrary bandwidths and shapes. Theoretically, we will show that MTRs utilize their degrees of freedom to uniquely match or exceed the performance obtained by all the conventional approaches. Practically, the self-aligned nature of MTRs not only reduces fabrication cost and complexity, but also enables higher precision and almost ideal performance predicted in theory, especially for larger number of layers.

An additional feature of MTRs is that they are easily applied on patterned substrates, including louvered wave plates [3, 21, 22], vector vortex-plates [23, 24], broadband polarization gratings [23, 25], and beyond. This will be the topic of a subsequent study.

Note that we explicitly allow a zero twist angle (*i.e.*, homogeneous) as one of the possible solutions of a twist layer. To be clear, we define an MTR as having two or more self-aligning layers wherein at least one has a non-zero twist - otherwise it would be entirely homogeneous.

#176332 - $15.00 USD Received 17 Sep 2012; revised 30 Nov 2012; accepted 3 Dec 2012; published 4 Jan 2013
(C) 2013 OSA

2.1. Materials

Since MTRs require multiple twisted birefringent layers, LCs which may be formed into polymer networks [26, 27] are ideal. LC polymers (LCPs), also called reactive mesogens, are initially low molecular weight LCs which may be aligned by surfaces [28] and inherent chirality [29] into complex profiles, as with conventional LCs, but which may then be cured into solid polymer films by photo-polymerization. A principle feature of MTRs is the propagating alignment from prior layers to subsequent - auto-cloned alignment. This occurs spontaneously for many layers provided the prior are well-ordered and polymerized.

While nearly any LCP may be employed for MTRs, we will here use RMS10-025 (Merck Chemicals Inc). This has a reported birefringence dispersion of $\Delta n(\lambda) = 0.128 + 8390/\lambda^2$, which we have experimentally also verified. We assume this real-world birefringence dispersion for all simulations here, in anticipation of the experimental results.

2.2. Theory

The basic unit cell of all MTRs is a single twisted birefringent layer (Fig. 2), which is well known [13]. While the total effect of the multiple twists is not trivial, its analysis is straightforward with standard transfer matrix techniques. For a given material, an MTR with M total layers has $2M+1$ parameters: each layer m has its own twist ϕ_m and thickness d_m, plus the start angle ϕ_0 of the first twist layer that is set by the alignment layer on the substrate. Using these constraints, the Mueller matrix $\mathbf{T}_m$ of any particular layer may be written as [13]

$$\mathbf{T}_m = \begin{pmatrix} 1 & 0 & 0 & 0 \\ 0 & 1-2(c^2+d^2) & 2(bd-ac) & -2(ad+bc) \\ 0 & 2(ac+bd) & 1-2(b^2+c^2) & 2(ab-cd) \\ 0 & 2(ad-bc) & -2(ab+cd) & 1-2(b^2+d^2) \end{pmatrix}, \text{with} \tag{1}$$

$$a = \cos X_m \cos\phi_m + \phi_m \sin\phi_m \operatorname{sinc} X_m, \tag{2}$$

$$b = -\zeta_m \cos\left(2m\overline{\phi} - \phi_m\right) \operatorname{sinc} X_m, \tag{3}$$

$$c = \cos X_m \sin\phi_m - \phi_m \cos\phi_m \operatorname{sinc} X_m, \tag{4}$$

$$d = -\zeta_m \sin\left(2m\overline{\phi} - \phi_m\right) \operatorname{sinc} X_m. \tag{5}$$

In the above, each layer has a normalized retardation $\zeta_m = \Gamma_m(\lambda)/2 = \pi\Delta n(\lambda) d_m/\lambda$, a parameter $X_m = \sqrt{\zeta_m^2 + \phi_m^2}$, and a biased mean $\overline{\phi} = (\sum_{i=0}^{m} \phi_i + \pi/2)/m$. The function $\operatorname{sinc} X_m = (\sin X_m)/X_m$. Our convention is that the optical axis is parallel to the LC nematic director; for positive Δn materials, this is the slow axis. The Mueller matrix of the whole MTR is therefore

$$\mathbf{T}_{MTR} = \mathbf{T}_M \cdots \mathbf{T}_2 \mathbf{T}_1, \tag{6}$$

and the output polarization may be found as $\mathbf{S}_o = \mathbf{T}_{MTR}\mathbf{S}_i$, where $\mathbf{S}_o(\lambda)$ and $\mathbf{S}_i(\lambda)$ are the output and input Stokes vectors for each wavelength, respectively. Note, $\mathbf{S} = (S_0, S_1, S_2, S_3)^T$ can be measured using several standard approaches [1]. Since MTRs by definition have an inhomogeneous profile of a uniaxial birefringence, they are in general neither uniaxial nor biaxial on the whole. Nevertheless, an effective retardation and an optical axis direction can be calculated for the entire structure by comparing the Stokes output to that expected from a standard homogeneous retarder, for the same input polarization.

2.3. MTR design

Designing an MTR involves choosing the $2M+1$ parameters. In principle, this might be done directly using the matrix $\mathbf{T}_{MTR}$. If a general polarization transformation problem involves a

#176332 - $15.00 USD Received 17 Sep 2012; revised 30 Nov 2012; accepted 3 Dec 2012; published 4 Jan 2013
(C) 2013 OSA

set of known input and desired output polarizations for N specific design wavelengths, then it might be possible to solve the system of equations arising from Eq. (6) to find viable exact MTR solutions when they exist. Even in the simplest case (*e.g.*, Appendix A), however, this involves long coupled implicit equations and requires numerical methods.

Therefore, we turn immediately to numerical optimization for almost all MTR designs, using Eq. (6). At a high level, this design process is simple: setup a cost function f, and search for its global (and sometimes local) minima. This cost function may be a function of the target $\mathbf{S}_t(\lambda)$ and the output $\mathbf{S}_o(\lambda)$ polarization spectrum of a particular solution (given a known input $\mathbf{S}_i(\lambda)$), or it may be a function of one of the components of $\mathbf{T}_{MTR}[row,col]$. Simple examples include $f = \overline{1-\mathbf{S}_o(\lambda)\cdot\mathbf{S}_t(\lambda)}$ and $f = \overline{1-|\mathbf{T}_{MTR}[4,2](\lambda)|}$. It is often desirable to apply a cost function that is even more nonlinear, so that the search converges more quickly, such as $f = \overline{1-|e(\lambda)|}$ where $e = \tan\left((\sin^{-1}S_3)/2\right)$ is the ellipticity [1]. Note that f may also be setup to include other constraints, *e.g.*, fabrication preferences or limitations. We often use Matlab™for the solution optimization, especially with `fminsearch`, but many other numerical tools could be just as easily employed. Multiple start points are generally needed.

Even within conservative bounds for d and ϕ, this optimization may lead to dozens of local minima, many of which are equivalent global minima with an approximately identical f result. In this underdetermined situation, we are free to rank and select convenient solutions.

We next derive optimal designs for quarter- and half-wave phase retarders. For simplicity and clarity, we study and demonstrate these elements for the visible wavelength region. Note, however, that designs for different wavelength ranges can be easily obtained by scaling the thicknesses of the individual layers without changing the twist angles.

3. Achromatic and super-achromatic quarter-wave MTRs

Quarter-wave (QW) retarders transform to/from linear (*e.g.*, $\mathbf{S}_i = (1,1,0,0)^T$) and circular (*e.g.*, $\mathbf{S}_t = (1,0,0,1)^T$) polarizations. In our formalism, this requires that $\mathbf{T}_{MTR}[2,2] = 0$, $\mathbf{T}_{MTR}[3,2] = 0$, and $\mathbf{T}_{MTR}[4,2] = 1$, exactly for specific wavelengths, or nearly so for a given bandwidth. We will divide our analysis in this section into two cases: achromatic MTRs with $M = 2$ layers, and super-achromatic MTRs with $M = 3$ layers. For convenience, we label these as 2TR and 3TR designs, respectively, and will adopt this notation generally for all MTRs.

3.1. Achromatic quarter-wave 2TRs ($M = 2$ layer designs)

Several notable 2TR achromatic QW designs exist. The cross-section for all 2TRs is illustrated in general in Fig. 3(a). The first and simplest solution may be found analytically, as described in Appendix A. Notwithstanding, this first and all other solutions can be found using numerical

Table 1. Summary of 2TR (achromatic) and 3TR (super-achromatic) QW designs.

DESIGN	$\phi_0(^\circ)$	$d_1(\mu\text{m})$	$\phi_1(^\circ)$	$d_2(\mu\text{m})$	$\phi_2(^\circ)$	$d_3(\mu\text{m})$	$\phi_3(^\circ)$	$\overline{e(\lambda)}$
2TR QW-A	14.3	1.18	0	1.13	83.5	-	-	0.97
2TR QW-B	0	1.90	25.2	0.96	79.3	-	-	0.97
2TR QW-C	65	0.93	18.8	1.28	−89	-	-	0.96
3TR QW-A	6.4	1.05	0	1.95	43.1	0.83	83.0	0.96
3TR QW-B	0	1.85	11.4	1.76	42.3	0.8	83.0	0.97

#176332 - $15.00 USD Received 17 Sep 2012; revised 30 Nov 2012; accepted 3 Dec 2012; published 4 Jan 2013
(C) 2013 OSA

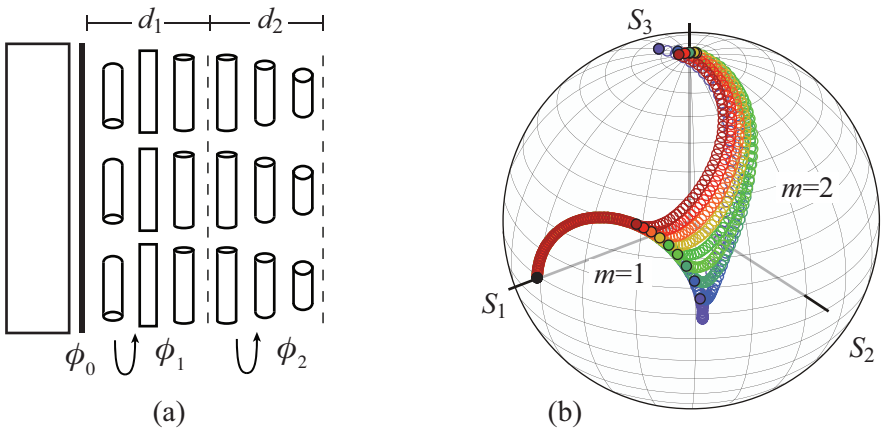

Fig. 3. (a) Illustration of the two layer MTR (2TR). (b) The polarization evolution within the 2TR QW-A design, on the Poincaré sphere (450 to 650 nm shown, spacing of 25 nm).

optimization of the cost function $f = \overline{1 - \mathbf{S}_o(\lambda) \cdot \mathbf{S}_t}$, within the bandwidth 450-650 nm.

The most simple design (2TR QW-A) was found by requiring that the first layer have zero-twist, along with a second non-zero twist layer; it should be the easiest to fabricate, and is the thinnest solution we could find. The next most preferable solution (2TR QW-B and 2TR QW-C) involves two non-zero twist layers, with the same and opposite chiral handedness, respectively. All of these designs are listed in Table 1, in ascending order of complexity.

The output of all 2TR QW designs for a linear (horizontal) input polarization is shown in Fig. 4. The output Stokes component $S_3 \sim 1$, ellipticity $e \sim 1$, and the effective net retardation $\sim 90^\circ$. Also shown is the comparison result from the traditional DP achromatic QW design [8] (*i.e.*, two homogeneous plates with thicknesses 1.75 and 0.88 μm, and with their optical axes oriented at 15° and 74°, respectively). These are all nearly identical. Note that the effective optical axis angle (Fig. 4(d)) is not exactly 45°, but close, as with nearly all approaches.

The Poincaré sphere helps explain how the 2TR QW functions. In Fig. 3(b) we show the polarization evolution through the thickness of the 2TR QW-A, across the 450-650 nm spectrum. In a novel way for compound retarders, the first layer of the 2TR QW design transforms the input linear polarization to a nontrivial elliptical polarization, which is then taken to the target circular polarization by the second. This is characteristically different than the path taken by the DP design [8], where the polarization states can be tracked analytically unlike in the case of MTRs. The MTR's additional degrees of freedom not available from conventional approaches allows more flexibility in tuning the final polarization spectral distribution, precisely because they access more possible polarization trajectories.

For our purposes here, we now define a normalized bandwidth for QW retarders as the approximate wavelength range for which $S_3 \geq 0.995$, and equivalently $e \geq 0.9$, divided by the center wavelength. This means that the 2TR QW designs have a normalized bandwidth of $\sim 37\%$. While this is useful for many applications, there are many situations when a wider bandwidth is needed. Fortunately, we can reach substantially wider bandwidths by adding additional layers, one of the most important features of the MTR family.

3.2. Super-achromatic quarter-wave 3TRs ($M = 3$ layer designs)

Here we describe several 3TR super-achromatic QW designs, with much wider bandwidths than the 2TR achromatic QW designs in the prior section. The cross-section for all 3TRs is illustrated in general in Fig. 5(a). We used the same numerical optimization approach and f as

#176332 - $15.00 USD Received 17 Sep 2012; revised 30 Nov 2012; accepted 3 Dec 2012; published 4 Jan 2013
(C) 2013 OSA

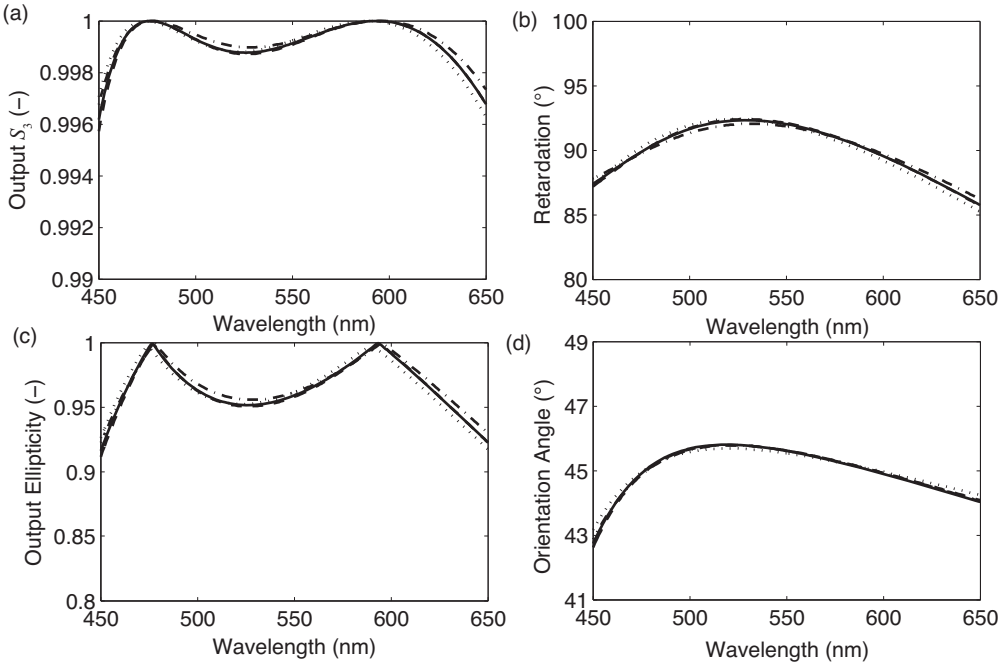

Fig. 4. Simulated output of the achromatic 2TR QW designs, and the comparative DP example, assuming a linear (horizontal) input: (a) Stokes S_3; (b) effective retardation; (c) ellipticity; and (d) effective optical axis orientation angle. Curves: QW-A (solid), QW-B (dashed), QW-C (dash dot), and DP (dotted).

Sec. 3.1, but across an increased wavelength range of 400 to 800 nm.

The most simple design (3TR QW-A) was found by requiring that the first layer have zero-twist, and allowing the other two to take any non-zero twist; it should be the easiest to fabricate. When we relaxed the zero-twist restriction, another solution resulted (3TR QW-B). These designs are listed in Table 1.

The output of all 3TR QW designs is shown in Fig. 6(a), with many similarities to the 2TR designs, but with a wider bandwidth. Also shown is the comparison result from the traditional Pancharatnam super-achromatic QW design [9] (*i.e.*, three homogeneous plates with thicknesses 1.6, 1.6, and 0.8 μm, and with their optical axes oriented at 7°, 27° and 65°, respectively). These are all again nearly identical.

In Fig. 5(b) we show the polarization evolution on the Poincaré sphere through the thickness of the 3TR QW-A, across a 425 to 775 nm spectrum. The first layer of the 3TR QW design fans out the polarizations, only moderately, near the input linear polarization. These are then transformed across the hemisphere by the second layer, and finally taken up to the pole by the third. This is characteristically different than the path taken by the Pancharatnam design [9], where the first two homogeneous HW retarders are aligned at specific angles such that they rotate the horizontal input to three polarization states that fall exactly along a meridian aligned at 45° to the third QW homogeneous retarder. These are distributed around the equator to exactly match the dispersion of the last retarder, which sends them to the pole [9].

The 3TR QW designs have a normalized bandwidth of $\sim$ 75%, a factor of two greater than the 2TRs. The trend with MTRs should be clear: the more layers that are added, the wider the bandwidth will be, with only minor added complexity.

#176332 - $15.00 USD Received 17 Sep 2012; revised 30 Nov 2012; accepted 3 Dec 2012; published 4 Jan 2013
(C) 2013 OSA

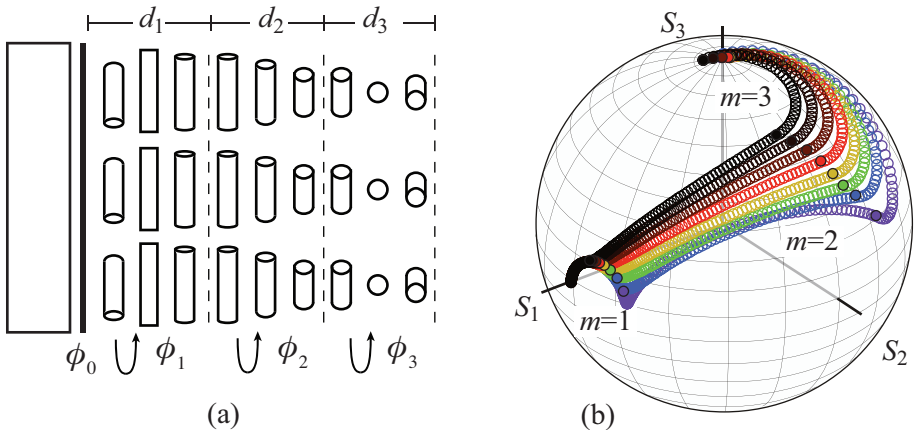

Fig. 5. (a) Illustration of the three layer MTR (3TR). (b) The polarization evolution within the 3TR QW-A design, on the Poincaré sphere (425 to 750 nm shown, spacing of 50 nm).

4. Achromatic and super-achromatic half-wave MTRs

Another important polarization element is the half-wave (HW) retarder, which transforms to/from linear to another (rotated) linear polarization (*lin-lin*), sometimes used to accomplish optical rotation. Similarly, HW retarders are sometimes used to transform circular to orthogonal circular (*cir-cir*) polarizations. Here we describe two classes of MTR HW designs that accomplish both transformations. The most preferable 2TR and 3TR designs were found for the bandwidths 450-650 nm and 400-800 nm, respectively, and are shown in Table 2. The following results show that the normalized bandwidths of 2/3TR HW designs are similar to the analogous QW MTRs (*i.e.*, 37% and 75%, for the achromatic 2TRs and super-achromatic 3TRs, respectively). In this HW case, the analogous normalized bandwidth definition is the wavelength range for which $|S_{(1 \text{ or } 3)}| \geq 0.99$, divided by the center wavelength.

4.1. *Achromatic and super-achromatic half-wave MTRs (*lin-lin*)*

Admittedly, a single twisted LC layer can accomplish rotation of linear polarizations over modest bandwidths when the Mauguin [13] condition is satisfied. However, MTRs can be used to achieve wider bandwidths at relatively smaller thicknesses. For *lin-lin* HW MTRs ("A" designs), we assumed a horizontal linear input polarization, and set the target output polarization as vertical linear (*e.g.*, $\mathbf{S}_t = (1,-1,0,0)^T$).

Table 2. Summary of 2TR and 3TR HW designs (*lin-lin* ="A" and *cir-cir* ="B").

DESIGN	$\phi_0(^\circ)$	$d_1(\mu\text{m})$	$\phi_1(^\circ)$	$d_2(\mu\text{m})$	$\phi_2(^\circ)$	$d_3(\mu\text{m})$	$\phi_3(^\circ)$	$\overline{\mathbf{S}^{(1 \text{ or } 3)}(\lambda)}$
2TR HW-A	−18.5	1.94	171	3.20	−62.4	-	-	−0.99
3TR HW-A	9.2	0.86	0	3.29	66.7	1.66	14.1	−0.99
2TR HW-B	−3.4	1.56	69.7	1.56	−69.7	-	-	−0.99
3TR HW-B	47.3	1.1	76.4	2.27	0	1.1	−76.4	−0.99

#176332 - $15.00 USD Received 17 Sep 2012; revised 30 Nov 2012; accepted 3 Dec 2012; published 4 Jan 2013
(C) 2013 OSA

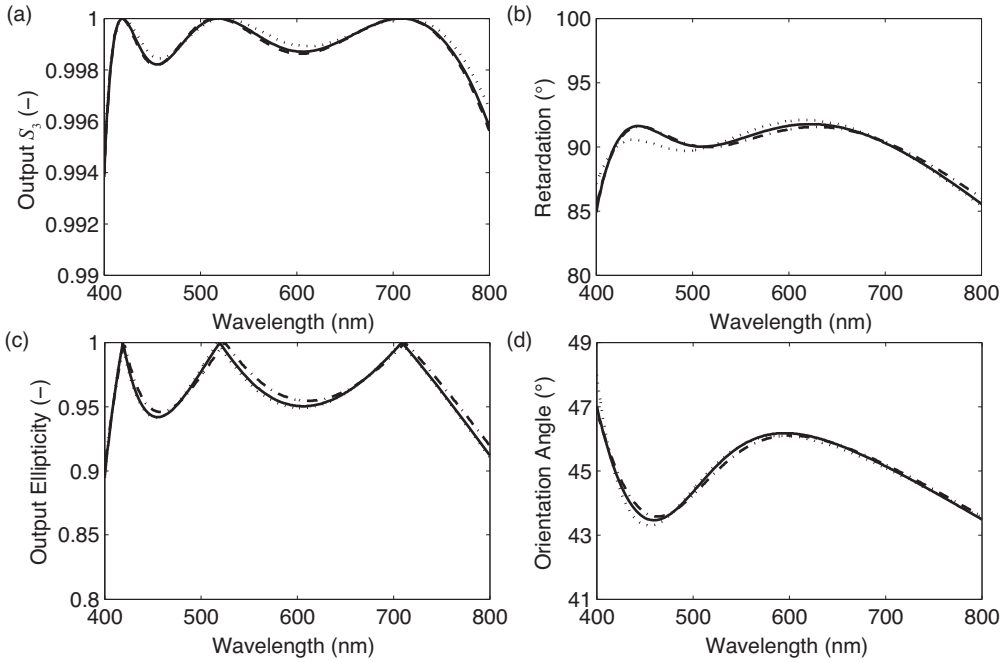

Fig. 6. Simulated output of the super-achromatic 3TR QW designs, and the comparative Pancharatnam example, assuming a linear (horizontal) input: (a) Stokes S_3; (b) effective retardation; (c) ellipticity; and (d) effective optical axis orientation angle. Curves: QW-A (solid), QW-B (dash dot), and Pancharatnam (dotted).

The output of the 2/3MTR HW (*lin-lin*) designs are shown in Fig. 7(a)-(b), where most notably the output Stokes component $S_1 \sim -1$ and retardation $\sim 180^\circ$. Also shown are the comparison results from a DP-type achromatic HW design [30] (*i.e.*, two homogeneous plates both with thicknesses 1.77 μm, and optical axes at 22.5° and 67.5°), and a Pancharatnam design (*i.e.*, three homogeneous plates with thicknesses 3.2, 1.6, and 1.6 μm, and optical axes at 19°, 93°, and 48°, respectively). We are not certain why these results do not better overlap the MTR output. Irregardless, the 2TR HW-A and 3TR HW-A designs achieve achromatic and super-achromatic HW behavior for *lin-lin* transformation.

*4.2. Achromatic and super-achromatic half-wave MTRs (*cir-cir*)*

Some elements require *cir-cir* HW transformation, including those operating on the Pancharatnam-Berry phase [23–25], and in many cases an achromatic effect is also desired. MTRs offer an elegant solution for this, despite the fact that a single twisted LC layer does not mimic a HW retarder for circularly polarized light (even at the Mauguin condition [13]). For *cir-cir* HW MTRs ("B" designs), we assumed a circular input polarization (*e.g.*, $\mathbf{S}_i = (1,0,0,1)^T$), and set the target output polarization as its orthogonal (*e.g.*, $\mathbf{S}_t = (1,0,0,-1)^T$).

The output of the 2/3MTR HW *cir-cir* designs are shown in Fig. 7(c)-(d), where most notably the output Stokes component $S_3 \sim -1$ and retardation $\sim 180^\circ$. Also shown are the comparison results of a Pancharatnam (QHQ) achromatic design [10] (*i.e.*, three homogeneous plates with thicknesses 0.83, 1.66, and 0.83 μm, with optical axes at 16°, 59.3°, and 16°, respectively), and another Pancharatnam design (*i.e.*, three homogeneous plates with thicknesses 0.81, 3.22, and 0.81 μm, with optical axes at 19.7°, 74.1°, and 19.7°, respectively). These overlap almost

#176332 - $15.00 USD Received 17 Sep 2012; revised 30 Nov 2012; accepted 3 Dec 2012; published 4 Jan 2013
(C) 2013 OSA

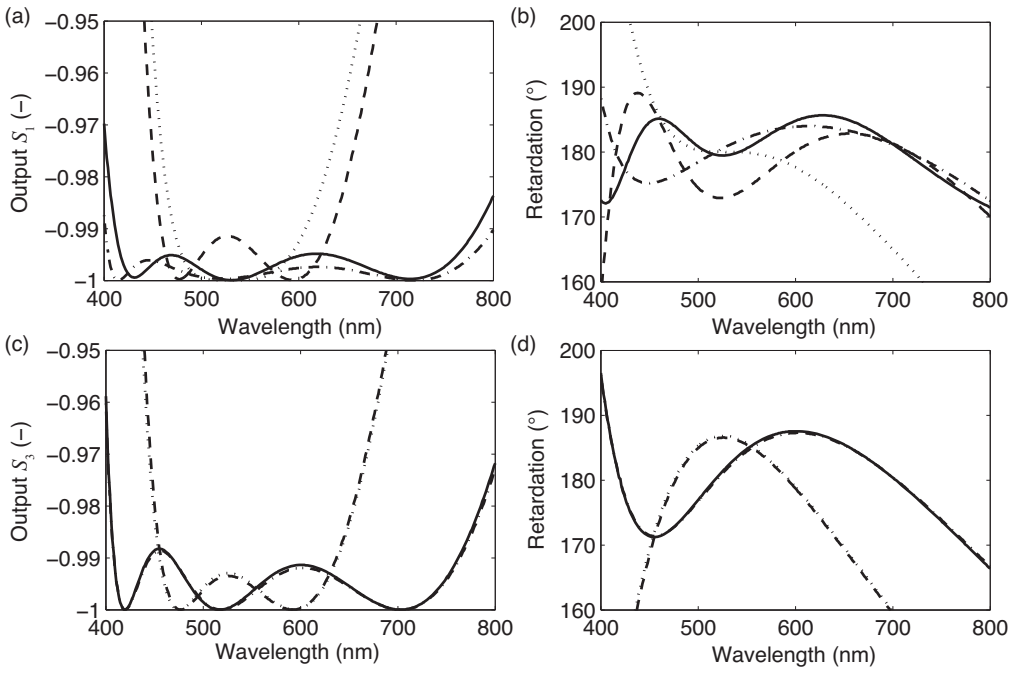

Fig. 7. Simulated output of the (achromatic) 2TR and (super-achromatic) 3TR HW designs, and their comparative Pancharatnam examples: (a) and (b) show the output for the *lin-lin* HW MTRs, with a linear (horizontal) input polarization; whereas (c) and (d) show the output from *cir-cir* HW MTRs, with a circular (right) input. Curves: 2TR (dashed), 3TR (bold), and corresponding Pancharatnam (dotted and dash dot, respectively).

exactly. In summary, the 2TR HW-B and 3TR HW-B designs achieve achromatic and super-achromatic HW behavior for *cir-cir* transformation.

5. Experimental validation

We now outline the essential MTR fabrication procedure, describe the specific experimental parameters we employed to generate several of the elements described above. We then characterize these samples and compare with both simulation and commercial alternatives. Our analysis reveals that MTRs are easily fabricated with standard tools and materials, and achieve excellent optical properties in all cases that correspond well to the simulations above.

5.1. Fabrication

In principle, MTR fabrication is as easy as coating at least three polymer layers, as shown in Fig. 8. First (a), the alignment layer is applied. Second (b), a layer of LCP is coated and allowed to align to the layer below. Third (c), the LCP layer is cured, usually by (UV) photo-polymerization, to form a cross-linked polymer network. Finally (d), one or more additional layers LCP are coated and cured, aligned by the top surface of the immediately prior LCP layer to orient its start angle, until the full MTR is completed. In practice, fabrication is quick (few minutes), very repeatable, and scalable to large areas - we routinely coat 2 to 6 inch diameter elements. We often laminate a glass endcap onto the exposed LCP final layer, for protection and anti-reflection effects.

For the results here, we used a photo-alignment material LIA-C001(DIC Corp), on borofloat

#176332 - $15.00 USD Received 17 Sep 2012; revised 30 Nov 2012; accepted 3 Dec 2012; published 4 Jan 2013
(C) 2013 OSA

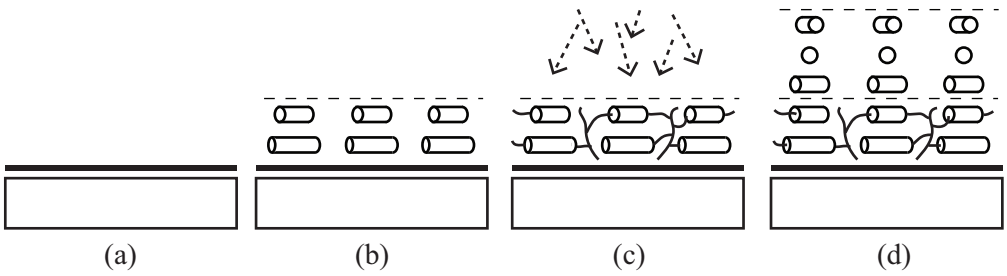

Fig. 8. The MTR fabrication procedure resulting in a monolithic broadband element, on a single substrate and alignment layer: (a) alignment layer processing; (b) LCP coating ($m = 1$); (c) LCP photo-polymerization; and (d) repeat LCP coating and curing for ($m \geq 2$).

glass (PG&O). Vendor-recommended processing was used (1500 rpm spin, then hotplate bake of 1 min at 100°C), and was then exposed to a UV LED source (0.5 J/cm^2, 365 nm, Clearstone Technologies) with linear polarizer arranged to set the desired ϕ_0. All subsequent LCP layers were based on RMS10-025 (discussed in Sec. 2.1), doped with various small amounts of chiral agents CB-15 and MLC-6247 (both Merck Chemicals Inc), which have positive and negative twist sense, respectively, along with a solvent PGMEA (Fisher Scientific). The LCP layers were photo-polymerized under a dry nitrogen environment, with the same unpolarized UV source and fluence as for the photo-alignment layer (but without the aforementioned polarizer). This fluence was sufficient to polymerize the LCP completely and prevent any dissolution from the mixtures of any subsequent layers. We found it convenient to develop several mixtures, as listed in Table 3, and used the spin recipes in Table 4. With our current processing, the tolerances on the twist angles and the thicknesses of the individual MTR layers are within 1°, and 25 nm respectively, which is sufficient for achieving excellent performance in the visible range.

Table 3. LCP mixtures for 2TR and 3TR QW designs.

MIX	Materials	wt : wt Ratio	Net Chiral : LCP-solids : Solvent
Raw-LCP	(set by vendor)	(set by vendor)	0 : 0.3 : 0.7
A	CB-15(+) : PGMEA	0.02: 0.98	0.02 : 0 : 0.98
B	MLC-6247(−) : PGMEA	0.02: 0.98	0.02 : 0 : 0.98
C	Mix-A : Raw-LCP	0.4 : 1	0.0057 : 0.21 : 0.79
D	Mix-A : Raw-LCP	0.05 : 1	0.0009 : 0.28 : 0.72
E	Mix-B : Raw-LCP	0.19 : 1	0.0032 : 0.25 : 0.75
F	Mix-A : Raw-LCP	0.13 : 1	0.0023 : 0.26 : 0.74
G	Mix-A : Raw-LCP	0.1 : 1	0.0018 : 0.27 : 0.73
H	Mix-A : Raw-LCP	0.47 : 1	0.0064 : 0.2 : 0.8

#176332 - $15.00 USD Received 17 Sep 2012; revised 30 Nov 2012; accepted 3 Dec 2012; published 4 Jan 2013
(C) 2013 OSA

Table 4. Recipes for the 2TR and 3TR QW designs.

DESIGN	Layer 1	Layer 2	Layer 3
2TR QW-A	raw-LCP, 1000 rpm	Mix-C, 800 rpm	-
2TR QW-B	Mix-D, 750 rpm	Mix-C, 1000 rpm	-
2TR QW-C	Mix-E, 600 rpm	Mix-F, 1500 rpm	-
3TR QW-A	raw-LCP, 2500 rpm	Mix-G, 500 rpm	Mix-H, 1300 rpm

5.2. Characterization

In order to characterize MTRs and other competitive samples, we constructed a simple measurement tool using linear polarizers (Edmund Optics Ltd) mounted within precision rotation stages (Thorlabs Ltd), and a high quality achromatic QW retarder (AQW2, Colorlink Japan, Ltd). In all cases, Stokes parameters were measured through a series of intensity measurements [1] collected by a spectrometer (Ocean Optics Ltd) across the desired wavelength range. The data was post-processed in MATLAB to estimate the Stokes parameters, and subsequently calculate relevant parameters including the effective retardation, effective optic axis orientation, and ellipticity. Our tool was calibrated using a known retarder, where we matched our measurement data to that supplied by the vendor within 1%, and we confirmed our measurements on a series of retarders using a commercial measurement tool (Axoscan). We then used this tool to optimize the individual chiral dopant concentrations listed in Table 3 until the desired performance was achieved from the respective MTR designs.

5.3. Results on achromatic and super-achromatic QW MTRs

The output from the fabricated QW MTRs is shown in Fig. 9. The measured retardation from the QW-A designs corresponds extremely well to the predicted spectra in Fig. 4(b) and 6(b). The least-squares best fit leads to estimated thicknesses and twists that are within $\pm$4% of the target values in Table 1 in all cases. As a baseline, we show the retardation of our own measurement on the commercial AQW2 retarder, and vendor-provided retardation of a commercial super-achromatic QW retarder (AQWO05M-600, Thorlabs).

The measured retardation for the 2TR QW-A sample in Fig. 9(a) are close to the desired value of 90° across the wavelength range of 450-650 nm. For horizontally polarized input, the average ellipticity of the output from this element was measured as $\overline{e(\lambda)} = 0.96$, indicating that the emerging light is almost perfectly circularly polarized. This is substantially the same as our measurement on the commercial AQW2 retarder. Although 2TR QW-A represents one of the simplest achromatic MTR-QW designs, we have elsewhere reported [21] similarly excellent results with both 2TR QW-B, and 2TR QW-C designs.

The measured retardation for the 3TR QW-A sample in Fig. 9(b) are close to the desired value of 90° across the much larger wavelength range of 400-800 nm. For horizontally polarized input, we measured the average output ellipticity as $\overline{e(\lambda)} = 0.95$. The fabrication process is similar to that of the 2TR QWPs, with the addition of just one extra twist layer. The 3TR QW-A sample also improves upon the performance of the commercial AQWO05M-600 retarder, whose retardation spectrum has a much wider deviation across the same wavelength range.

#176332 - $15.00 USD Received 17 Sep 2012; revised 30 Nov 2012; accepted 3 Dec 2012; published 4 Jan 2013
(C) 2013 OSA

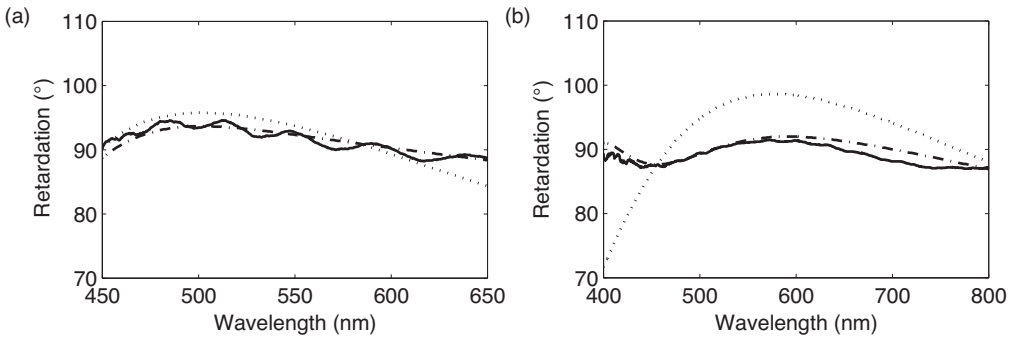

Fig. 9. Measured retardation spectra fabricated MTR QW elements, with linear (horizontal) input polarization. (a) Achromatic 2TR QW-A (solid) output, with the best fit simulation (dash dot), and the comparison AQW2 film (dotted) measured in the same way; (b) Super-achromatic 3TR QW-A (solid) output, with the best fit simulation (dash dot), and the comparison AQWO05M-600 element (dotted) from vendor-measured data.

5.4. Results on achromatic HW MTRs

Elsewhere, we have reported some experimental results on fabrication of (*cir-cir*) HW elements, and specifically the 2TR HW-B design [23] developed earlier for achromatic polarization gratings [25]. Note that although the context is different, the performance achieved from these elements match the simulations presented in this manuscript. The processing instructions reported earlier can be applied to other HW applications as well. We are presently working on 3TR HW designs for broader bandwidth and will report on these results later.

6. Discussion

MTRs represent a new family of phase retarders that can be designed for general polarization manipulation, and are substantially easier to fabricate than prior methods.

In order to highlight the performance trends of MTRs, we compare their normalized bandwidths in Fig. 10 to several popular achromatic retarders. We use the normalized bandwidth ($\Delta\lambda/\lambda_0$) definitions for QW and HW in Sec. 3; the precise bandwidth depends on the birefringence dispersion of the particular material being used, but it is nearly always close to these results. As already proven, as M increases, so does the normalized bandwidth. Beyond this, the general lesson is that each comparison retarder (*i.e.*, formed with multiple homogeneous plates) has an analogous MTR with the same number of layers with an equivalent normalized bandwidth. Note furthermore that the 4/5TR normalized bandwidths are larger than any we can find in the literature, and seem especially well-suited to short-, mid-, and long-wave infrared wavelengths.

One of the more recent advances in achromatic retardation is the development of a LC mixture which manifests a negative dispersion in the material itself [3]. While this does achieve some bandwidth enhancement (*i.e.*, compared to nearly all other materials) in an single layer, the normalized bandwidth remains modest at $\sim 15\%$. As shown in Fig. 10, this is around half the normalized bandwidth of the 2TR. Furthermore, the optimal wavelength range is limited by the chemistry, which is not easily extended to wider normalized bandwidths or into the infrared. However, it should be noted that these two approaches are not mutually incompatible - one could employ the negative dispersion LC within an MTR configuration, and achieve an even more functional retarder.

It is worthwhile to clarify some aspects of MTRs, which may not be evident in our dis-

#176332 - $15.00 USD Received 17 Sep 2012; revised 30 Nov 2012; accepted 3 Dec 2012; published 4 Jan 2013
(C) 2013 OSA

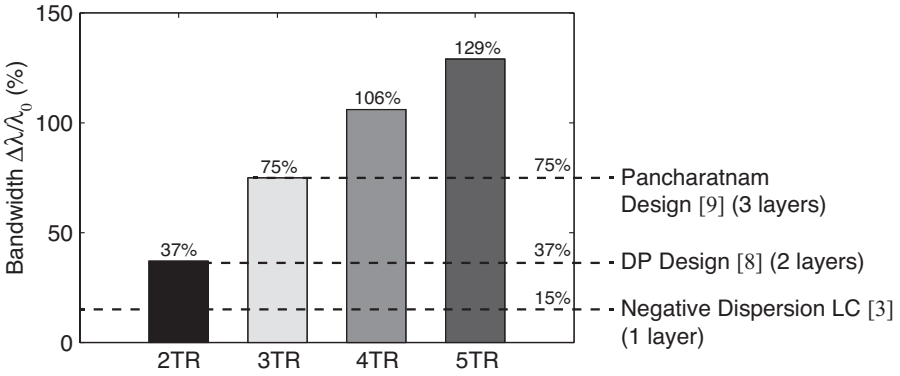

Fig. 10. Normalized bandwidth of achromatic MTRs (both QW and HW), and comparative examples in the prior art based on homogenous plates.

cussion so far. Due to their inhomogeneous nature, the MTR designs in general (and many of the comparison examples discussed above) do not have a true optical axis, a direction along which polarization is preserved. Note that if indeed such a behavior is desired, it is possible to accomplish this in MTRs using additional layers analogous to the Pacharatnam QHQ [10] design. Consequently, care must be taken when reversing the input and output sides of the particular MTR designs presented here. For example, the 2TR QW-A design will transform linear to circular polarizations when the input side is layer 1, and circular to linear when the input side is layer 2. However, if circular is input into layer 1, then the output will not be linear.

Another important property of MTRs is their acceptance angle (*i.e.*, angular aperture). Our preliminary simulations and experimental observations suggest that the QW and HW MTRs discussed above behave uniformly within at least 30° incident angle.

Although we describe implementing MTRs with LCs, it should be clear that the optical principles remain the same, even if an alternative birefringent means is employed, including form-birefringence, metamaterials, nano-particles/wires/tubes, and beyond.

Finally, because of their self-aligning behavior, it is straightforward to apply MTRs onto patterned substrates, to enable complex birefringent optics [23–25]. In many of these cases, it is cumbersome or even impossible to apply the conventional achromatic retarder approaches. Indeed, this was a primary motivation to develop MTRs, and has resulted in their use within a new polarization conversion system [22] for highly efficient portable projectors.

7. Conclusion

We have identified an agile new approach for achieving broadband retarders using multiple twisted birefringent layers on a single substrate. When formed with chiral LCs, these layers are self-aligning, use a single alignment layer, and are dramatically easier to fabricate compared to prior approaches with multiple homogeneous retarders. We analyze MTR optics with Mueller calculus, and describe a numerical design method to obtain several MTR designs for QW and HW retardations. The performance of these (bandwidth, effective retardation, and orientation angles) matches or exceeds that possible through conventional approaches. We validated many of the QW designs by fabricating high quality MTRs using standard materials and processing, that achieve excellent achromatic operation at visible wavelengths. These results compare very favorably with corresponding commercial products that are relatively expensive and/or involve complex manufacturing.

#176332 - $15.00 USD Received 17 Sep 2012; revised 30 Nov 2012; accepted 3 Dec 2012; published 4 Jan 2013
(C) 2013 OSA

A. Appendix

A.1. Exact solution method for achromatic quarter-wave 2TRs

In general, the design of MTRs cannot be done analytically, since the functional dependence of $\mathbf{T}_{MTR}$ on the design parameters d_m and ϕ_m is so nonlinear. However, it is possible to find exact solutions of $3N$ implicit equations that derive from $\mathbf{T}_{MTR}$ for N wavelengths. While our preferable design approach involves minimizing a cost function dependent on the Mueller matrix elements, described in Sec. 2.3, we here describe an alternative exact solution procedure.

The only case that appears to permit a tractable discussion is the 2TR where we assume that the first layer has zero twist angle $\phi_1 = 0$. Four design parameters must be found: the two thicknesses d_1 and d_2, the second layer twist angle ϕ_2, and the starting orientation angle ϕ_0.

We begin by identifying two design wavelengths λ_1 and λ_2, at which the 2TR outputs exactly circular polarization for a linear input. In our formalism, this requires the following to be true at both wavelengths:

$$\mathbf{T}_{2TR}[2,2] = (1-2(c_2^2+d_2^2))(1-2d_1^2) + 4b_1d_1(b_2d_2 - a_2c_2) - 4a_1d_1(a_2d_2 + b_2c_2) = 0 \quad (7)$$

$$\mathbf{T}_{2TR}[3,2] = 2(a_2c_2 + b_2d_2)(1-2d_1^2) + 2b_1d_1(1-2(b_2^2+c_2^2)) + 4a_1d_1(a_2b_2 - c_2d_2) = 0 \quad (8)$$

$$\mathbf{T}_{2TR}[4,2] = 2(a_2d_2 - b_2c_2)(1-2d_1^2) - 4b_1d_1(a_2b_2 + c_2d_2) + 2a_1d_1(1-2(b_2^2+d_2^2)) = 1 \quad (9)$$

where $a_1 = \cos\zeta_1$, and $c_1 = 0$ since $\phi_1 = 0$.

This is a system of linear equations with three unknowns ($1-2d_1^2$, $2b_1d_1$, and $2a_1d_1$). Using Cramer's rule involving determinants, the following simplified expressions result:

$$1 - 2d_1^2 = 2(a_2d_2 - b_2c_2) \quad (10a)$$

$$2b_1d_1 = -2(a_2b_2 + c_2d_2) \quad (10b)$$

$$2a_1d_1 = 1 - 2b_2^2 - 2d_2^2 \quad (10c)$$

These can be combined to arrive at the following implicit equations:

$$\sin 2\phi_0(\text{Eq.}(10a)) + \cos 2\phi_0(\text{Eq.}(10b)) \Rightarrow \quad \sin 2\phi_0 \cos 2\zeta_1 = 2\zeta_2 \operatorname{sinc} 2X_2 \quad (11a)$$

$$\cos 2\phi_0(\text{Eq.}(10a)) - \sin 2\phi_0(\text{Eq.}(10b)) \Rightarrow \quad \cos 2\phi_0 = 2\zeta_2\phi_2 \operatorname{sinc}^2 X_2 \quad (11b)$$

$$\text{Eq.}(10c) \Rightarrow \quad 1 - \sin 2\phi_0 \sin 2\zeta_1 = 2\zeta_2^2 \operatorname{sinc}^2 X_2 \quad (11c)$$

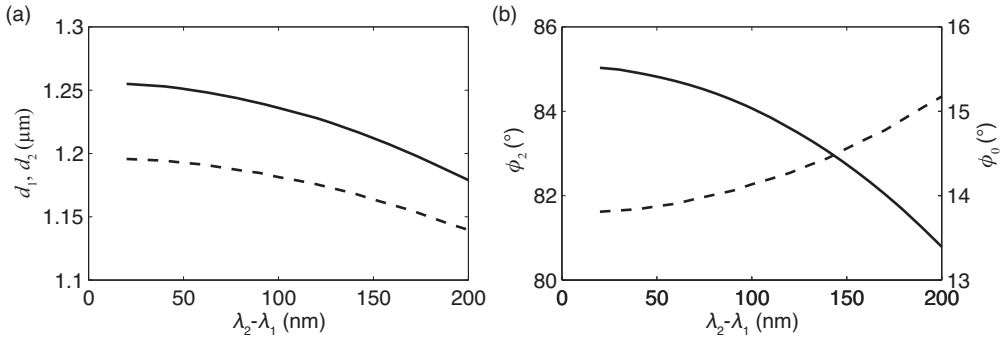

Fig. 11. Analytic estimation of 2TR QW-A design parameters. In part (a), the thicknesses of the first (bold) and second (dashed) layers are shown, while in part (b) the twist angle (bold) of the second layer and the start angle (dashed) have been calculated.

#176332 - $15.00 USD Received 17 Sep 2012; revised 30 Nov 2012; accepted 3 Dec 2012; published 4 Jan 2013
(C) 2013 OSA

Since these must be true for both design wavelengths, we have six implicit equations and four unknowns. There are various approaches to find solutions, but all of them involve at least some iterative numerical method. One approach is to solve the whole system of equations simultaneously (*e.g.*, using `fminsearch` in Matlab™); another approach is to algebraically manipulate the implicit equations to isolate and solve for just one unknown at a time (*e.g.*, using `fzero`).

Using this latter approach, we determined the solutions for a range of $\lambda_2 - \lambda_1$, centered around 550 nm. These are shown in Fig. 11. The 2TR QW-A design described in Sec. 3.1 is indicated. The main lesson is that a 2TR design may always be found for a given design wavelength separation $\lambda_2 - \lambda_1$. It is also interesting to note that the solutions smoothly vary.

Acknowledgments

The authors acknowledge the financial support of ImagineOptix Corp for this work. We also gratefully acknowledge ColorLink Japan Ltd for helpful discussions and independent measurements, and Merck Chemicals Ltd for access and advice on the RMS materials.

#176332 - $15.00 USD Received 17 Sep 2012; revised 30 Nov 2012; accepted 3 Dec 2012; published 4 Jan 2013
(C) 2013 OSA